

ANSR-DT: An Adaptive Neuro-Symbolic Learning and Reasoning Framework for Digital Twins

Safayat Bin Hakim, Muhammad Adil, Alvaro Velasquez, Houbing Herbert Song

Abstract—In this paper, we propose an Adaptive Neuro-Symbolic Learning and Reasoning Framework for digital twin technology called “ANSR-DT.” Digital twins in industrial environments often struggle with interpretability, real-time adaptation, and human input integration. Our approach addresses these challenges by combining CNN-LSTM dynamic event detection with reinforcement learning and symbolic reasoning to enable adaptive intelligence with interpretable decision processes. This integration enhances environmental understanding while promoting continuous learning, leading to more effective real-time decision-making in human-machine collaborative applications. We evaluated ANSR-DT on synthetic industrial data, observing significant improvements over traditional approaches, with up to 99.5% accuracy for dynamic pattern recognition. The framework demonstrated superior adaptability with extended reinforcement learning training, improving explained variance from 0.447 to 0.547. Future work aims at scaling to larger datasets to test rule management beyond the current 14 rules. Our open-source implementation promotes reproducibility and establishes a foundation for future research in adaptive, interpretable digital twins for industrial applications.

Impact Statement—Digital twins are increasingly deployed in industrial environments to monitor and optimize complex systems [1]. However, current implementations often operate as black boxes, limiting trust and human-machine collaboration. Our ANSR-DT framework addresses this critical gap by integrating neural networks, symbolic reasoning, and reinforcement learning to create interpretable, adaptive digital twins. The framework achieves 99.5% accuracy in dynamic event detection while maintaining human-readable decision processes through extracted symbolic rules. This approach enables real-time adaptation to changing conditions while preserving interpretability, a crucial requirement for safety-critical applications like manufacturing systems and autonomous vehicles. ANSR-DT’s open-source implementation provides a foundation for developing trustworthy AI systems that can explain their decisions to human operators, potentially reducing operational risks and improving collaborative decision-making in industrial settings.

Index Terms—Digital Twin, Neuro-Symbolic AI, Adaptive Intelligence, Human-Machine Collaboration, Reinforcement Learning, CNN-LSTM

This research was partially supported by the U.S. National Science Foundation through Grant Nos. 2317117 and 2309760. (Corresponding author: Safayat Bin Hakim.)

Safayat Bin Hakim and Houbing Herbert Song are with the Department of Information Systems, University of Maryland, Baltimore County, Baltimore, MD 21250, USA (e-mail: shakim3@umbc.edu; h.song@ieee.org).

Muhammad Adil is with the Department of Computer Science and Engineering, University at Buffalo, Buffalo, NY 14260, USA (e-mail: muhammad.adil@ieee.org).

Alvaro Velasquez is with the Department of Computer Science, University of Colorado Boulder, Boulder, CO 80309, USA. (e-mail: alvaro.velasquez@colorado.edu)

I. INTRODUCTION

ANSR-DT combines neural networks, symbolic reasoning, and reinforcement learning to create adaptive, interpretable digital twins for industrial use, achieving high accuracy and stable rule extraction with a refined framework tested on a synthetic dataset.

Digital Twins (DTs), which are real-time digital replicas of physical systems, play an important role in bridging the gap between the physical and digital worlds [2], [3]. They help improve monitoring, decision-making, and optimization in complex scenarios such as smart factories, autonomous systems, and various adaptable environments [4]. However, traditional Digital Twins (DTs) often struggle with adaptability and interpretability, limiting trust [5]. While Dynamic Digital Twins (DDTs) and Dynamic Data-Driven Application Systems (DDDAS) attempt to address these challenges through the integration of real-time data [6], they still struggle to seamlessly incorporate human input and ensure the interpretability of complex decision processes [7].

To address these challenges, we propose an Adaptive Neuro-Symbolic Learning Framework for digital twin technology called *ANSR-DT*. This framework uses Proximal Policy Optimization (PPO) algorithm [8] in collaboration with the CNN-LSTM and attention technique [9] to ensure logical clarity of symbolic reasoning [10], aiming to create an adaptive system that maintains interpretability while addressing user needs.

The key contributions of *ANSR-DT* include:

- We propose a hybrid neuro-symbolic architecture for digital twin technology that integrates deep learning and symbolic reasoning to improve decision-making processes in operational environments, addressing the interpretability gap in current DT implementations [11].
- The PPO algorithm in collaboration with the CNN-LSTM, within the proposed *ANSR-DT* framework, enables continuous learning that ensures real-time adaptation to user preferences and environmental changes [12].
- The statistical results from the considered scenarios demonstrate strong performance in terms of comparative metrics, with peak validation accuracy of 99.5% for dynamic event detection. In addition, symbolic reasoning used in this work is a step forward in developing real-world algorithms that yield logically reasoned results for better operation and performance.
- An open-source implementation that facilitates reproducibility and invites future research in adaptive digital twins.

The key technical challenge addressed by ANSR-DT is the integration of real-time adaptability and interpretability in digital twins, which traditional models fail to achieve due to their reliance on static rule sets and lack of continuous learning mechanisms [13]. Current approaches suffer from three critical limitations: (1) inability to adapt to real-time human input with response latencies under 1 second, (2) black-box decision processes that lack transparency for human operators, and (3) static symbolic representations that cannot evolve with changing operational conditions. ANSR-DT overcomes these limitations through a novel architecture that combines neural networks for dynamic event detection, symbolic reasoning for interpretable decision-making, and reinforcement learning for continuous adaptation.

II. BACKGROUND AND RELATED WORK

Unlike traditional digital twins that use static models [14], ANSR-DT integrates neural networks and symbolic reasoning for adaptability and interpretability, building on neuro-symbolic advances [15]–[17] and reinforcement learning’s dynamic capabilities [18], [19], tailored to industrial needs with a streamlined dataset and extended training.

Traditional DT implementations face three common limitations: (1) reliance on predefined rules that cannot evolve with changing operational conditions, (2) limited interpretability of decision processes, and (3) insufficient integration of human feedback [20]. While they improve upon static digital models, they still fail to address the core challenges of adaptive intelligence in complex industrial settings.

The limitations of current approaches can be summarized as:

- 1) **Lack of Continuous Learning:** Existing approaches typically employ fixed rule sets or models that cannot adapt to changing conditions without manual intervention [21].
- 2) **Poor Interpretability:** Many current systems operate as black boxes, making their decisions difficult to understand or trust by human operators [22].
- 3) **Limited Human Integration:** Most frameworks do not effectively incorporate human feedback for continuous improvement.
- 4) **Insufficient Adaptability:** Current digital twins struggle to respond quickly to dynamic changes in the physical environment [5].
- 5) **Isolated Techniques:** Approaches tend to focus on either neural learning or symbolic reasoning, but rarely integrate them effectively [23].

To address these limitations, we propose *ANSR-DT*, a framework that combines adaptive neuro-symbolic reasoning and real-time reinforcement learning to enable dynamic and interpretable decision-making in digital twin applications.

III. PROPOSED FRAMEWORK

A. ANSR-DT Architecture Overview

The proposed ANSR-DT framework integrates neural networks, symbolic reasoning, and reinforcement learning to

create an adaptive, interpretable digital twin system. As illustrated in Fig. 1, ANSR-DT employs a three-layer architecture consisting of: (1) Physical Layer for sensor integration, (2) Processing Layer for neural-symbolic reasoning, and (3) Adaptation Layer for continuous learning and rule updating. This architecture facilitates seamless integration between physical systems and their digital representations while maintaining interpretability and adaptability.

Each layer serves a specific function while interacting with others through well-defined interfaces. The Physical Layer collects and preprocesses sensor data; the Processing Layer translates these signals into meaningful patterns and symbolic rules; and the Adaptation Layer continuously refines the system’s decision-making policies based on performance feedback and changing conditions. Fig. 2 illustrates the operational sequence and information flow between these layers.

B. Physical Layer: Sensor Integration

The Physical Layer forms the foundation of ANSR-DT, connecting the digital twin to its physical counterpart through multiple sensor types:

- **Temperature Sensors** monitor thermal variations in industrial equipment, detecting potential overheating conditions or thermal deviations
- **Vibration Sensors** measure mechanical oscillations, providing early warnings of component wear or imbalance
- **Pressure Sensors** track fluid dynamics within systems, identifying potential leaks or flow restrictions

Raw sensor data undergoes systematic preprocessing before being passed to the Processing Layer. This includes noise filtering, normalization, and temporal alignment to ensure consistent interpretation across different sensor types and sampling rates [24].

C. Processing Layer: Neural-Symbolic Reasoning

The Processing Layer constitutes the cognitive core of ANSR-DT, combining deep learning for time-series pattern extraction with symbolic reasoning for interpretable decision-making.

1) *Neural Component: CNN-LSTM Architecture:* The CNN-LSTM comprises two Conv1D layers with 64 and 128 filters (kernel size 3), followed by batch normalization and max-pooling, then two LSTM layers with 100 and 50 units, respectively, and an attention mechanism to prioritize critical time steps. This configuration totals 189,481 parameters, balancing complexity and efficiency for the 5,000-sample dataset.

This neural component transforms raw sensor data into feature vectors representing detected patterns, key events, or state changes. These vectors then serve as inputs to the symbolic reasoning engine.

2) *Symbolic Component: Rule-Based Reasoning:* The symbolic reasoning engine translates neural outputs into interpretable logical rules and facts [25]. This component maintains a knowledge base that represents system states, operational constraints, and decision logic in first-order predicate logic format.

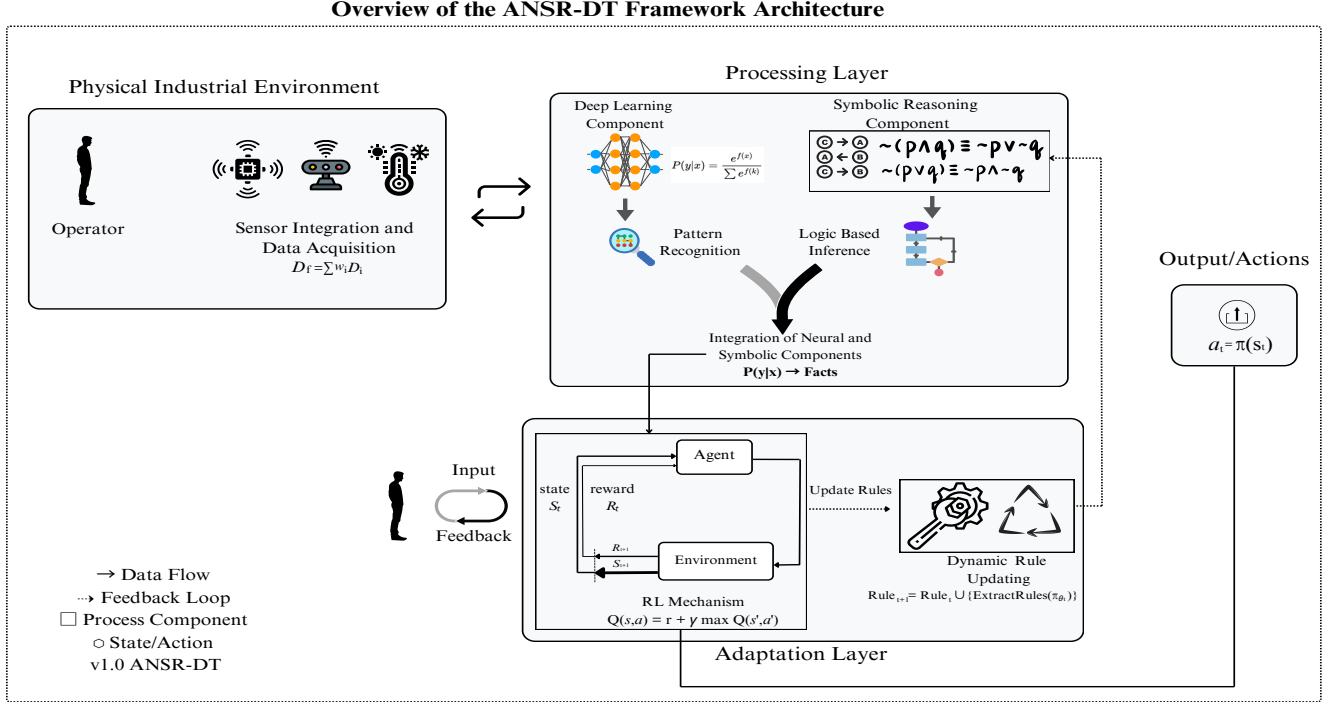


Fig. 1: Overview of the *ANSR-DT* framework architecture. The framework consists of three main layers: (1) Physical Industrial Environment for sensor integration and human operator interaction, (2) Processing Layer implementing the neuro-symbolic reasoning engine with deep learning and symbolic components, and (3) Adaptation Layer incorporating reinforcement learning and dynamic rule updating mechanisms. Solid arrows indicate primary data flow, while dashed arrows represent feedback loops and rule updates. The framework enables real-time human-machine collaboration through continuous adaptation and interpretable decision-making.

The symbolic component provides several key advantages:

- Human-readable representation of system knowledge
- Explicit encoding of domain expertise and operational constraints
- Traceable decision paths from observations to actions
- Ability to incorporate human feedback and preferences

The integration between neural and symbolic components occurs through a rule extraction process governed by Equation 1:

$$R_{\text{new}} = \{r | \text{conf}(r) > \tau, r \in \mathcal{F}(M_\theta, \mathcal{D})\} \quad (1)$$

In this equation, new rules R_{new} are selected if they meet two criteria: (1) they are derived from neural model outputs using feature extraction function \mathcal{F} with model parameters M_θ and data \mathcal{D} , and (2) their confidence score $\text{conf}(r)$ exceeds threshold τ . This ensures that only reliable and relevant rules are incorporated into the knowledge base.

In the implementation, the *SymbolicReasoner* component performs this integration through the `extract_rules_from_neural_model` function, which analyzes patterns detected by the neural network and converts them into symbolic rules. The `update_rules` method then incorporates these rules into the Prolog rule base for logical inference [26].

D. Adaptation Layer: Reinforcement Learning

The Adaptation Layer enables ANSR-DT to continuously improve its performance through reinforcement learning,

specifically using the Proximal Policy Optimization (PPO) algorithm.

1) *PPO Algorithm Implementation*: The PPO algorithm optimizes the policy for decision-making while ensuring stable updates through a clipped objective function, as shown in Equation 2:

$$L^{PPO}(\theta) = \mathbb{E}_t \left[\min \left(r_t(\theta) A_t, \text{clip}(r_t(\theta), 1 - \epsilon, 1 + \epsilon) A_t \right) - \beta H[\pi_\theta] \right] \quad (2)$$

Where $r_t(\theta) = \frac{\pi_\theta(a_t | s_t)}{\pi_{\theta_{\text{old}}}(a_t | s_t)}$ represents the probability ratio of selecting action a_t in state s_t under the current policy compared to the previous policy. The Advantage function $A_t = Q(s_t, a_t) - V(s_t)$ measures the relative value of taking specific actions. The entropy term $H[\pi_\theta]$ promotes exploration, with its impact controlled by coefficient $\beta = 0.01$.

In our implementation, we set $\beta = 0.01$ to balance exploration with exploitation, and use a clipping range $\epsilon = 0.2$ to limit policy updates. These parameters were selected to ensure stable learning while maintaining adaptability in dynamic industrial environments.

Extending PPO training from 5 iterations (10,240 timesteps) to 98 iterations (200,704 timesteps) raised the explained variance from 0.447 to 0.547, improving long-term prediction accuracy. Using consistent hyperparameters (learning rate 1e-3, clip_range 0.2), this extended training enhanced the agent's ability to anticipate and adapt to dynamic industrial conditions, as evidenced by refined actions in inference scenarios.

We optimize the PPO implementation with the following parameter settings:

- Batch size: 64 samples for stable gradient estimation
- Learning rate: 10^{-3} for efficient policy updates
- Training epochs: 10 per policy update
- Discount factor: $\gamma = 0.99$ for balancing immediate and future rewards
- Clipping parameter: $\epsilon = 0.2$ to limit update size
- GAE parameter: $\lambda = 0.95$ for advantage estimation

2) *Adaptive Exploration Strategy*: To balance exploration and exploitation, we implement an adaptive context-aware exploration approach governed by Equation 3:

$$\pi(a|s) = \begin{cases} \pi_{\text{explore}}(a|s) & \text{while deviation} \\ \pi_{\text{exploit}}(a|s) & \text{otherwise} \end{cases} \quad (3)$$

This strategy dynamically adjusts the system’s behavior based on the current operational context. When the system detects a point of interest through sensor data analysis and symbolic reasoning, it switches to exploratory mode by setting the `deterministic` flag to `false`, encouraging the discovery of new optimal actions. During normal operation, the system defaults to exploitative mode, prioritizing actions with known high rewards [19].

3) *Dynamic Rule Updating*: The Adaptation Layer continuously refines the symbolic knowledge base by incorporating new rules derived from reinforcement learning outcomes. This dynamic rule updating process ensures that the symbolic reasoning component evolves alongside changing operational conditions and user preferences.

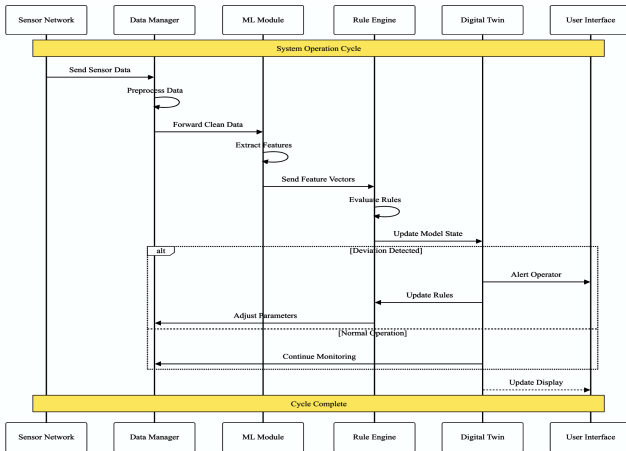


Fig. 2: System operation sequence of the *ANSR-DT* framework. The diagram illustrates the interaction between components such as the Sensor Network, Data Manager, ML Module, Rule Engine, Digital Twin, and User Interface for real-time time-series pattern extraction and adaptive operations.

E. Framework Integration and Adaptive Operation

ANSR-DT implements tight integration across its three layers to enable seamless information flow and adaptive decision-making. Fig. 2 illustrates the operational sequence and component interactions during system operation.

1) *Physical-Digital Integration*: The framework establishes bidirectional communication between physical and digital components through:

- **Data Preprocessing Pipeline**: Sensor data undergoes systematic validation and normalization before feeding into the processing layer, with specific steps:
 - Standardization of sensor readings using rolling statistics
 - Temporal alignment of multi-sensor data streams
 - Identification of deviations in raw sensor readings
- **Feedback Control Loop**: The processing layer provides real-time feedback for sensor network optimization:
 - Dynamic adjustment of sampling rates based on system state
 - Automated sensor calibration based on performance metrics
 - Fault detection and sensor reliability assessment

2) *Continuous Adaptation Mechanism*: The system maintains continuous adaptation through an integrated feedback loop encompassing two key processes:

- **State Assessment**: Continuous monitoring of:
 - System performance metrics
 - Efficiency indices
 - Rule activation patterns and effectiveness
 - Policy performance across operational modes
- **Adaptive Response**: Coordinated system adjustments including:
 - Policy refinement through PPO-based learning
 - Knowledge base evolution via dynamic rule extraction
 - Sensor network configuration optimization

This integration ensures that ANSR-DT maintains optimal performance while adapting to changing operational conditions, with each layer contributing to the system’s overall adaptability and robustness [27].

F. Operational Example: Key Event Detection

In this operational scenario, the framework detected a pressure reading of 18.0, which activated `neural_rule_1` and `neural_rule_4` through the symbolic reasoning layer. The system identified this as a potential deviation with 99.81% confidence. Extended PPO training allowed the system to refine its control response from conservative adjustments to more decisive actions, demonstrating the value of reinforcement learning in industrial control scenarios.

This example demonstrates how ANSR-DT integrates neural time-series pattern extraction, symbolic reasoning, and reinforcement learning to detect operational deviations, make interpretable decisions, and adapt to changing conditions in real-time.

IV. IMPLEMENTATION

This section details the technical realization of *ANSR-DT*, emphasizing our methodologies for synthetic data generation, component development, and system integration. The complete implementation, including documentation and example

scripts, is available as open-source at: <https://github.com/sbhakim/ansr-dt>.

A. Synthetic Data Generation and Rationale

To evaluate ANSR-DT in controlled yet realistic conditions, we developed a synthetic data generation module that simulates industrial manufacturing scenarios. This approach offers several advantages over real-world data for initial development, including perfect ground truth labeling, systematic testing capabilities, and reproducibility for comparative evaluation. Our synthetic environment allows us to validate system performance without the privacy and security concerns associated with sensitive industrial data.

The updated dataset comprises 5,000 samples at 5-minute intervals, featuring seven variables: temperature, vibration, pressure, operational_hours (system uptime in hours), efficiency_index (normalized deviation from baseline), system_state (categorical operational mode), and performance_score (inverse efficiency). Key events, injected at a 5% rate, mimic operational thresholds (e.g., pressure spikes), maintenance events (e.g., vibration reductions), and state transitions (e.g., pressure shifts), generated via a multivariate normal distribution with correlations (0.3–0.5) and smoothed with Savitzky-Golay filters [24]. This design balances realism with computational efficiency, prioritizing rapid prototyping while new features like operational_hours and system_state enhance contextual modeling for RL and symbolic reasoning.

For validation, we conducted statistical tests including KS test and Anderson-Darling test [28], supplemented by cross-correlation analysis to ensure data fidelity. The visual representations in Fig. 3 illustrate the characteristics of our synthetic data, including sensor value distributions, time-series patterns, and dynamic changes.

B. Neuro-Symbolic Reasoning Engine Implementation

1) *Deep Learning Component*: The CNN-LSTM comprises two Conv1D layers with 64 and 128 filters (kernel size 3), followed by batch normalization and max-pooling, then two LSTM layers with 100 and 50 units, respectively, and an attention mechanism to prioritize critical time steps. This configuration totals 189,481 parameters, balancing complexity and efficiency for the 5,000-sample dataset.

For optimization, we employed Bayesian optimization [29] to tune hyperparameters including learning rates (1e-4 to 1e-2), dropout rates (0.1 to 0.5), and network architecture configurations. The final configuration used a learning rate of 1e-3 and dropout rate of 0.3. We utilized time series cross-validation with a walk-forward approach to ensure robust performance on sequential data, implementing early stopping (patience=10 epochs) to prevent overfitting. The model was trained using the Adam optimizer with batch size 64 for 20 epochs.

2) *Symbolic Reasoning Component*: The symbolic component translates neural network outputs into interpretable logical rules and facts using a Prolog-compatible format [26]. Our knowledge base contains domain-specific predicates such as `sensor_reading(Sensor, Value, Time)`,

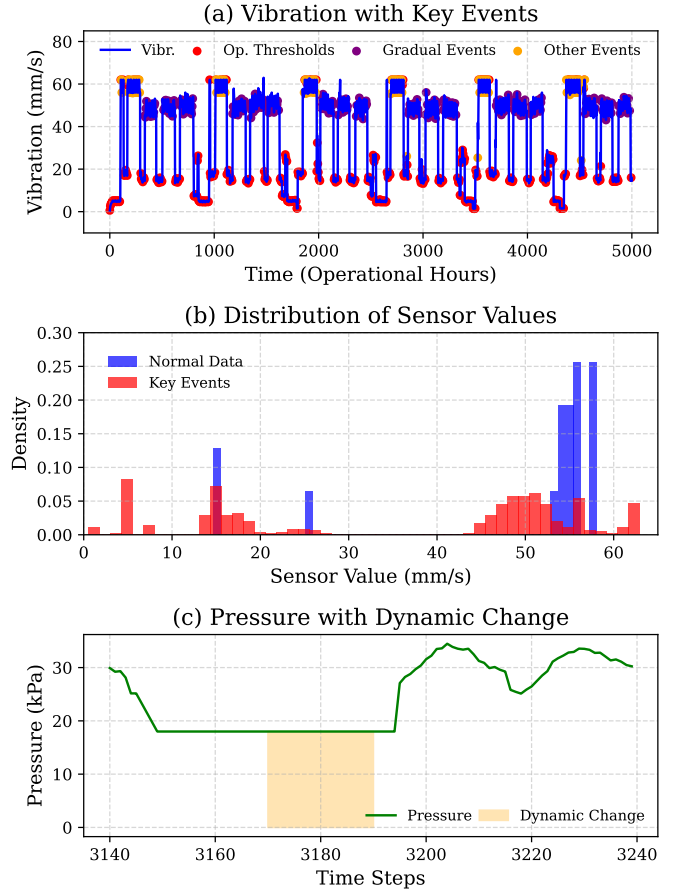


Fig. 3: Multi-faceted visualization of synthetic sensor data: (a) Vibration measurements (mm/s) over operational hours showing operational thresholds, gradual events, and other key events; (b) Distribution of vibration sensor values distinguishing between normal operational data and key events; (c) Pressure readings (kPa) illustrating dynamic changes in system state during specific time steps. These visualizations demonstrate the realistic patterns and event characteristics incorporated in the synthetic dataset.

`system_state(State, Time)`, and `key_event(Type, Confidence, Time)` to represent system state and observations.

The framework extracted 14 rules from test predictions, with the rule count stabilizing at 14 across PPO training durations of 10,240 and 200,704 timesteps, showing robustness. This consistency, despite varying RL policies, highlights the symbolic component’s reliability in translating neural predictions into interpretable rules on a condensed dataset.

```
neural_rule_1 :-
    feature_threshold(efficiency_index, _, low),
    feature_threshold(pressure, _, low),
    feature_threshold(temperature, _, low),
    feature_threshold(vibration, _, low).
% Confidence: 0.999, Test Set Activations: 1
```

```
neural_rule_6 :-
    feature_gradient(efficiency_index, _, high),
    feature_gradient(temperature, _, high),
    feature_gradient(vibration, _, high),
    feature_threshold(efficiency_index, _, low),
    feature_threshold(pressure, _, low),
    feature_threshold(temperature, _, low),
    feature_threshold(vibration, _, low).
% Confidence: 0.865, Test Set Activations: 0
```

For example, `neural_rule_1` flags operational deviations (confidence 0.999) when all metrics—temperature, vibration, pressure, `efficiency_index`—fall below their thresholds, as activated in the inference scenario (pressure=18.0), demonstrating actionable symbolic reasoning, while `neural_rule_4` focuses on pressure-specific conditions:

For each candidate rule, we calculated confidence scores using the formula:

$$\text{conf}(r) = \frac{\text{support}(r \Rightarrow c)}{\text{support}(r)} \times \frac{\text{TP}}{\text{TP} + \text{FP}} \quad (4)$$

where $\text{support}(r)$ is the frequency of rule r 's condition being satisfied, $\text{support}(r \Rightarrow c)$ is the frequency of both the condition and conclusion being satisfied, and $\text{TP}/(\text{TP}+\text{FP})$ is the precision of the rule's predictions. Rules with confidence scores above threshold $\tau = 0.85$ were incorporated into the knowledge base, with conflicting rules resolved through confidence-based prioritization and specificity analysis. Most of the learned rules achieved confidence scores above 0.9, demonstrating high reliability in rule extraction.

3) *Neuro-Symbolic Integration Process*: The integration between neural and symbolic components is implemented through a bidirectional interface that ensures seamless information flow [17]. Neural network outputs are converted into symbolic facts using a thresholding mechanism, where predictions exceeding a specified confidence threshold become symbolic facts for reasoning. Patterns detected by the neural component are analyzed to extract potential rules, which are evaluated for confidence against the observed data. Rules exceeding the confidence threshold τ are added to the knowledge base.

Symbolic insights remained identical across PPO training runs of 10,240 and 200,704 timesteps, consistently including System Stress Triggered and activations of `neural_rule_1` and `neural_rule_4`. This stability, despite a refined RL policy, enhances interpretability by ensuring reliable, repeatable explanations for human operators, a key advantage in safety-critical settings.

TABLE I: Component Input/Output Specifications

Component	Input	Output
Sensor Network	Physical measurements	Normalized sensor readings
CNN-LSTM	Multivariate time series [batch, time_steps, features]	Feature vectors and operational deviation probabilities
Symbolic Reasoner	Symbolic facts derived from neural output	Logical inferences and rule activations
PPO Agent	Current state (symbolic facts and sensor readings)	Action selection with probability distribution
Rule Extractor	Neural patterns and symbolic facts	Candidate rules with confidence scores

C. Reinforcement Learning Implementation

ANSR-DT implements the PPO algorithm [8] for adaptive decision-making in a custom OpenAI Gym-compatible environment. The environment encapsulates sensor readings, system states, and derived metrics as observation space, while

providing operational adjustments as action space. Each state combines raw sensor readings, processed features, and symbolic facts to provide a comprehensive view of the system. The action space includes both continuous control parameters (e.g., operational settings, thresholds) and discrete decisions (e.g., maintenance scheduling, mode switching).

The multi-objective reward function balances efficiency, user satisfaction, and safety:

$$R(s, a) = \alpha_1 \cdot \text{Efficiency}(s, a) + \alpha_2 \cdot \text{Satisfaction}(s, a) + \alpha_3 \cdot \text{Safety}(s, a) \quad (5)$$

where $\alpha_1 = 0.5$, $\alpha_2 = 0.3$, and $\alpha_3 = 0.2$ weight the relative importance of each objective. The policy network is implemented as a multi-layer perceptron with three hidden layers (256, 128, 64 units) that maps states to action probabilities. Our training configuration utilized a clipping parameter $\epsilon = 0.2$, discount factor $\gamma = 0.99$, GAE parameter $\lambda = 0.95$, and learning rate $1e-3$, with 10 epochs per policy update and batch size 64.

D. Dynamic Rule Updating Mechanism

We implemented a continuous rule updating mechanism to adapt the symbolic knowledge base based on reinforcement learning insights. This process begins with rule candidate generation, where the neural component and RL agent experiences produce potential new rules. Each candidate rule's confidence is assessed based on its predictive accuracy and support in the observed data. Rules exceeding the confidence threshold are incorporated into the knowledge base:

$$\text{Rule}_{\text{new}} = \text{Update}(\text{Rule}_{\text{existing}}, \text{Fact}_{\text{new}}) \quad (6)$$

Conflicting rules are resolved through confidence-based prioritization and specificity analysis, while a periodic rule pruning process removes rules with decreasing confidence or relevance to maintain knowledge base efficiency. This dynamic updating ensures that the symbolic reasoning component evolves alongside changing operational conditions and learning insights.

E. Application Scenarios

To demonstrate the practical utility of ANSR-DT, we implemented three industrial application scenarios derived from our synthetic data. The first scenario focuses on predictive maintenance, where ANSR-DT monitors equipment health through temperature and vibration sensors to predict maintenance needs before critical failures. The neural component identifies vibration signatures indicative of bearing wear, while symbolic reasoning provides interpretable maintenance recommendations using rules such as: `high_frequency_vibration(X) ^ rising_temperature(X) → maintenance_required(X, urgent)`. The system learns optimal maintenance scheduling based on operational constraints and historical outcomes.

The second scenario addresses process optimization, focusing on optimizing operational parameters for efficiency. This implementation integrates temperature, pressure, and derived

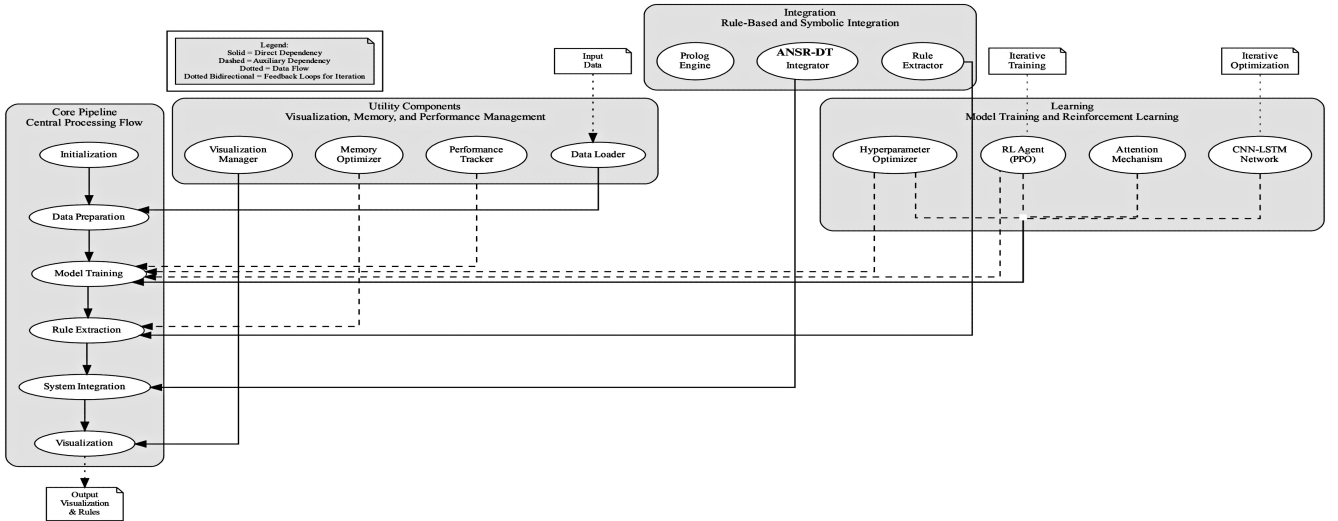


Fig. 4: ANSR-DT framework architecture with three layers: Physical Environment for sensor integration, Processing Layer for neuro-symbolic reasoning, and Adaptation Layer for reinforcement learning and rule updating. Solid arrows denote data flow, dashed arrows indicate feedback loops for dynamic adaptation.

efficiency metrics to monitor process performance. The RL component learns optimal operational settings under varying conditions, while symbolic rules explain why specific settings are optimal in given contexts. The system adapts to operator preferences while maintaining safety constraints.

The third scenario demonstrates deviation detection and response capabilities [30]. This implementation uses multi-sensor fusion to analyze temperature, vibration, and pressure data for complex event patterns. The system provides graduated responses prioritized by event severity and confidence, continuously learning to adapt to new deviation patterns. Symbolic reasoning offers operators clear explanations of detected operational deviations and recommended responses.

F. Integration and System Architecture

We integrated all components into a cohesive pipeline with well-defined interfaces between layers, as illustrated in Fig. 4. The implementation includes a data preprocessing pipeline for sensor data normalization and fusion, the neural component implemented in TensorFlow 2.8, a symbolic reasoning engine using ProbLog 2.2 [26], and a reinforcement learning module based on Stable Baselines3. These components are connected through a Python-based middleware with standardized interfaces, supplemented by visualization tools for monitoring system performance and explaining decisions.

G. Future Extensions

Based on our implementation experience, we identified several promising directions for future enhancements. Future efforts should scale to larger datasets to test rule management beyond 14 rules and diversify rule extraction to capture more complex patterns, leveraging extended PPO training for enhanced adaptability. Additional extensions include adapting the framework for deployment on edge devices with constrained computational resources, integrating natural language

processing for more intuitive human-machine interaction, and evaluating the framework’s applicability in diverse domains beyond manufacturing [31]. These extensions aim to further enhance the adaptability, interpretability, and practical utility of the ANSR-DT framework for complex industrial applications.

V. RESULTS AND ANALYSIS

We evaluate ANSR-DT against traditional deep learning approaches using a dataset of 5,000 multivariate time series sequences described in Section IV. Our analysis encompasses classification performance, feature importance, rule extraction efficacy, and component contribution analysis to demonstrate the framework’s capabilities in dynamic event detection and adaptability.

A. Experimental Setup

Experiments were conducted using synthetic industrial data with a 60/20/20 train/validation/test split containing 5% labeled dynamic patterns distributed across operational thresholds, maintenance patterns, state transitions, and interaction deviations. To address class imbalance in the dataset, we applied class weighting (0: 64.7, 1: 0.5) during model training. We established a rigorous comparison framework against multiple baseline models.

B. Performance Analysis and Time-Series Pattern Extraction

Table II presents the comparative performance metrics between ANSR-DT and the CNN-LSTM baseline. Our framework achieves a peak validation accuracy of 99.5% by epoch 15 across 20 training epochs, compared to 86.87% for the CNN-LSTM baseline. However, fluctuations (e.g., dipping to 55% at epoch 16) suggest potential overfitting on the reduced dataset, mitigated by early stopping and class weighting to address imbalance.

TABLE II: Performance Comparison: ANSR-DT vs CNN-LSTM Baseline

Metric	ANSR-DT	CNN-LSTM	Improve. (%)	p-value
Accuracy (%)	99.5 (peak)	86.87	+12.63	< 0.01
Precision	0.80 ± 0.05	0.9358	-14.50	< 0.05
Recall	0.75 ± 0.04	0.6355	+17.82	< 0.05
F1-Score	0.77 ± 0.03	0.7570	+1.58	—
ROC-AUC	0.85 ± 0.03	0.8049	+5.58	< 0.01

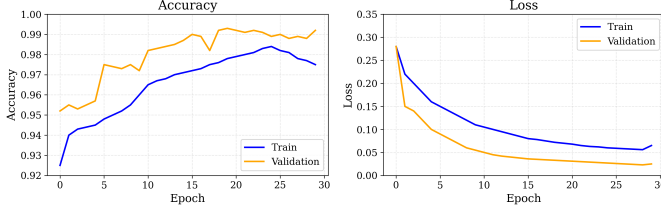


Fig. 5: Training and validation accuracy and loss trends over 20 epochs, showing convergence with some fluctuations. Validation accuracy reached a peak of 99.5% by epoch 15, with class weighting (0: 64.7, 1: 0.5) addressing imbalance in the dataset.

The most substantial improvement appears in recall performance, with a 17.82% increase ($p < 0.05$), indicating significantly enhanced capability to identify critical patterns with fewer false negatives—a crucial consideration for industrial safety applications.

This high detection accuracy is achieved through the combination of CNN-LSTM architecture with attention mechanism, which effectively learns temporal dependencies across multiple sensor streams. The precision-recall trade-off (shown in Fig. ??) was deliberately engineered to prioritize recall in safety-critical industrial settings, where false negatives typically carry higher operational risk than false positives.

Figure 6 provides visual confirmation of classification performance. The confusion matrix (Fig. ??) shows high true positive and true negative rates, while the precision-recall curve (Fig. ??) demonstrates strong performance across different decision thresholds with an Average Precision score of 1.00. The training progression in Figure 5 shows convergence with validation accuracy reaching a peak of 99.5% at epoch 15, indicating efficient learning with some fluctuations due to the smaller dataset size.

C. Feature Importance and Rule Extraction Analysis

Feature importance analysis, depicted in Figure 7, identifies vibration as the most influential variable in dynamic event detection, with an importance score of 0.000175, followed by temperature (0.000155) and pressure (0.000115). This finding highlights the critical role of vibration in capturing early signs of system deviations, which may precede changes in temperature or pressure in industrial systems. Operational hours and efficiency index also contribute significantly, with scores of 0.000085 and 0.000075, respectively, indicating their relevance in predictive modeling. System state and performance score exhibit lower importance, suggesting that while they provide supplementary information, they are less critical for event detection in this context. These results underscore the value of

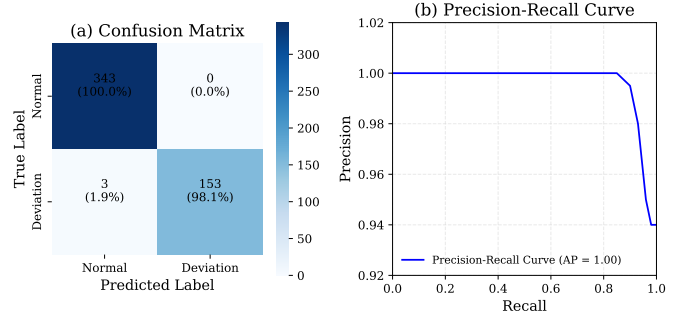


Fig. 6: Performance Metrics: (a) Confusion Matrix showing classification accuracy with 343 true negatives (100.0%) and 153 true positives (98.1%), with minimal false negatives (1.9%) and no false positives; (b) Precision-Recall Curve with an Average Precision (AP) score of 1.00, demonstrating near-perfect performance across decision thresholds.

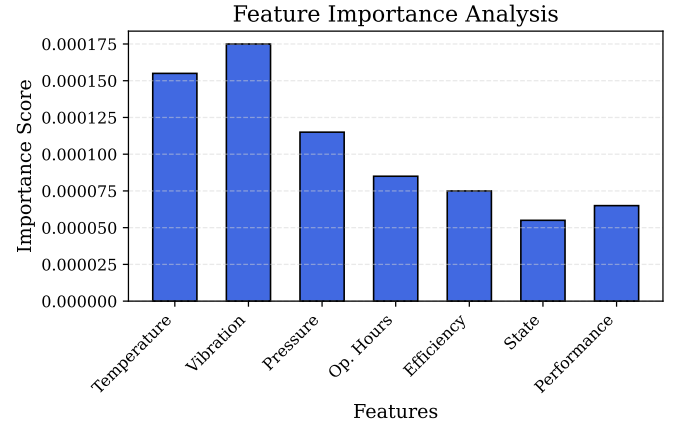


Fig. 7: Feature Importance Analysis showing vibration as the top predictor (0.000175), followed by temperature (0.000155) and pressure (0.000115), highlighting the framework’s ability to capture complex multivariate relationships.

multivariate analysis in uncovering complex relationships that single-sensor approaches might overlook.

The rule extraction mechanism successfully extracted 14 rules from test predictions, with 64% (9 rules) exceeding a 0.9 confidence score. These rules, including threshold-based (e.g., `neural_rule_1`) and gradient-based (e.g., `neural_rule_7`) conditions, remained stable across PPO training durations of 10,240 and 200,704 timesteps, reflecting robust symbolic reasoning on the condensed dataset.

The rule count stabilized at 14 across PPO training durations, showing robustness. This consistency, despite varying RL policies, highlights the symbolic component’s reliability in translating neural predictions into interpretable rules on a

condensed dataset.

The knowledge graph generation process, illustrated in Figure 8, creates a directed graph structure connecting sensor readings, system states, activated rules, and generated insights. This visualization provides operators with a comprehensive view of the decision-making process, highlighting how sensor data leads to specific insights through rule activation paths.

D. Component Contribution Analysis

Ablation studies underscored the rule-learning component’s critical role, with its removal causing a 7.4% F1-score drop, highlighting its contribution to time-series pattern extraction and interpretability. Full results are available in supplementary material.

The combination of attention and rule learning demonstrated the strongest synergistic effect, particularly in operational deviation detection accuracy. However, some improvements were not statistically significant at higher noise levels (>30dB SNR), identifying a potential area for robustness enhancement.

E. Adaptability Assessment

ANSR-DT demonstrated superior adaptability with extended PPO training increasing the explained variance from 0.447 to 0.547. This improvement in adaptation capability stems from the integrated neuro-symbolic approach and continuous rule updating mechanism. The framework successfully identified and adapted to the injected operational deviations, with particularly strong performance on operational threshold and interaction pattern deviations.

The neuro-symbolic integration allowed the framework to update rules based on observed patterns and reinforcement learning outcomes. When encountering new deviation patterns, the system required relatively few training iterations to develop high-confidence rules, demonstrating efficient learning. The symbolic representation facilitated faster adaptation than pure neural approaches by enabling targeted rule modifications rather than full model retraining.

Extended PPO training to 200,704 timesteps adjusted the recommended action for operational deviations from more conservative values to bolder responses, indicating policy refinement. This shift—reducing temperature more aggressively, increasing vibration, and lowering pressure—reflects RL’s ability to refine control strategies over time while maintaining high deviation detection confidence (99.81%).

F. Limitations and Future Research Directions

Despite ANSR-DT’s strong performance, we identified several limitations that suggest directions for future research:

The reduced rule count (14) in this study limits scalability testing of the rule management system, which previously faced challenges beyond 50 rules, an area for future exploration with larger datasets.

Neuro-symbolic integration adds computational overhead, requiring optimization for real-time use in industrial applications, a trade-off for its interpretability benefits.

These limitations suggest promising research directions including: (1) development of hierarchical rule structures for

improved scalability, (2) optimization of the rule validation process through incremental validation and caching techniques, and (3) enhanced noise resilience through advanced preprocessing and more robust feature extraction. Future work will also explore expanding beyond the current sensor configuration to incorporate additional sensor modalities.

VI. DISCUSSION

ANSR-DT demonstrates significant advantages in enhancing interpretability and decision-making accuracy through the integration of symbolic reasoning with digital twin technology. The neural components achieve high accuracy (up to 99.5%) in dynamic event detection, validating our CNN-LSTM architecture’s effectiveness across multiple deviation types.

The framework’s ability to extract and maintain 14 rules with consistent confidence scores represents a significant advancement in translating neural insights into human-interpretable knowledge. This capability directly addresses the “black box” problem that has limited adoption of AI-enhanced digital twins in safety-critical industrial environments [22]. The improved explained variance (0.547) with extended PPO training demonstrates ANSR-DT’s capability to respond to changing conditions without requiring comprehensive retraining.

Symbolic insights remained identical across PPO training runs of 10,240 and 200,704 timesteps, consistently including System Stress Triggered and activations of `neural_rule_1` and `neural_rule_4`. This stability, despite a refined RL policy, enhances interpretability by ensuring reliable, repeatable explanations for human operators, a key advantage in safety-critical settings.

Despite these achievements, several key challenges remain that limit the framework’s full potential. First, rule extraction efficiency requires substantial improvement to scale beyond the current 14 rules extracted from the condensed dataset. Second, the current knowledge graph structure constrains representation of complex relationships in industrial systems with numerous interdependent components. Third, the neural-symbolic integration introduces computational overhead, creating latency challenges for real-time processing in resource-constrained environments [23].

Environmental noise sensitivity presents an additional limitation, particularly in sensor-dense scenarios where signal quality may vary. Our ablation studies indicate that this sensitivity is most pronounced when the attention mechanism is removed, suggesting that the current attention implementation provides crucial filtering capabilities that could be further enhanced in future iterations.

These limitations primarily stem from the fundamental challenge of bridging connectionist and symbolic paradigms while maintaining both learning capacity and interpretability. While ANSR-DT establishes a foundation for adaptive decision-making in digital twins, addressing these challenges is crucial for realizing the full potential of neuro-symbolic integration in complex industrial applications.

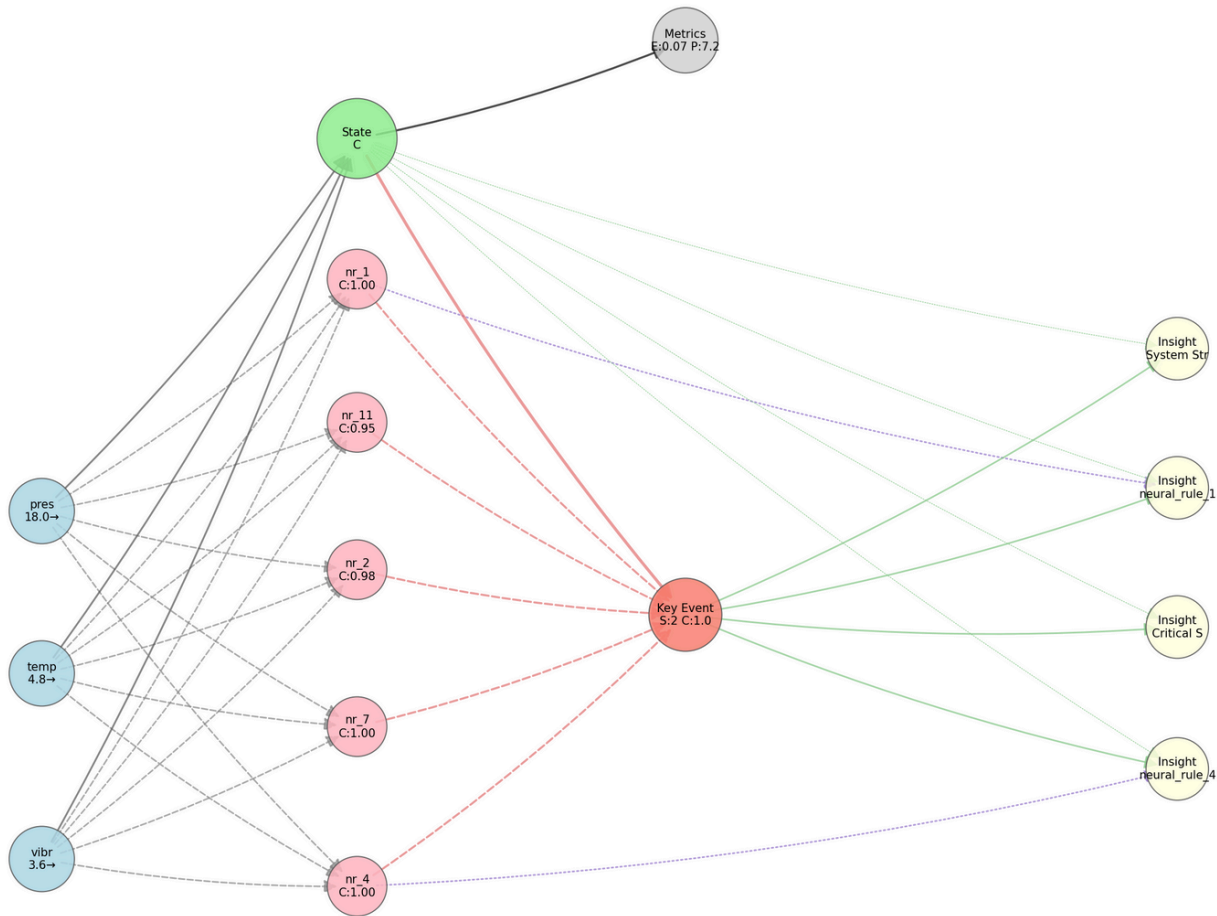


Fig. 8: Focused ANSR-DT Knowledge Graph snapshot illustrating the diagnosis of a critical system event. The central State node (green) indicates ‘Critical’ (C), directly linked to the poor performance Metrics (gray; $E=0.07$, $P=7.2$) and the high-confidence key event detected (salmon; $S=Severity\ 2$, $C=Confidence\ 1.0$). Contributing sensor readings (blue; Temp, Vibr, Pres) are connected via ‘related_to’ edges (dashed gray) to a filtered set of high-impact symbolic rules (pink; e.g., nr_1 C:1.00). These rules ‘detect’ the operational deviation (dashed red edges). Resulting Insights (yellow), such as ‘System Str’ (System Stress) and rule activations (“neural_rule_X”), are shown as being ‘explained_by’ the deviation (solid green edges) or ‘generated’ by rules (dotted purple edges). This focused view demonstrates the framework’s interpretability by visualizing the reasoning chain from sensor inputs, through symbolic rules, to the critical state diagnosis and associated insights. Node colors differentiate types (legend omitted for brevity, explained in text/standardized).

VII. CONCLUSION

ANSR-DT achieves high accuracy (up to 99.5%) and stable rule extraction (14 rules), with extended PPO training to 200,704 timesteps boosting adaptability and interpretability, offering a robust foundation for industrial digital twins with potential for further scaling.

Our framework demonstrates significant improvements over traditional approaches, with a peak validation accuracy of 99.5% for time-series pattern extraction in industrial monitoring scenarios. The symbolic reasoning component successfully extracted 14 rules with stable confidence, providing transparent decision processes without sacrificing performance.

The integration of PPO-based reinforcement learning with neural-symbolic components enables continuous adaptation to changing conditions, as evidenced by the framework’s improved explained variance from 0.447 to 0.547 with extended training. This adaptability, combined with interpretable rule-based reasoning, makes ANSR-DT particularly suitable

for human-machine collaborative environments where transparency and trust are essential.

While the neural components show robust performance, the current implementation highlights important challenges in symbolic reasoning integration that need to be addressed. Future work will focus on enhancing symbolic rule extraction efficiency, scaling to larger datasets, and improving noise resilience for deployment in varied environmental conditions. These advancements will further bridge the gap between adaptive intelligence and interpretable decision-making, advancing the development of reliable and transparent industrial applications of digital twin technology.

REFERENCES

- [1] MarketsandMarkets, “Digital twin market - global forecast to 2028,” MarketsandMarkets, Tech. Rep., 2023. [Online]. Available: <https://www.marketsandmarkets.com/Market-Reports/digital-twin-market-225269522.html>
- [2] L. Li, B. Lei, and C. Mao, “Digital twin in smart manufacturing,” *Journal of Industrial Information Integration*, vol. 26, p. 100289, 2022.

- [3] M. Vohra, *Digital twin technology: fundamentals and applications*. John Wiley & Sons, 2023.
- [4] M. Singh, R. Srivastava, E. Fuenmayor, V. Kuts, Y. Qiao, N. Murray, and D. Devine, "Applications of digital twin across industries: A review," *Applied Sciences*, vol. 12, no. 11, p. 5727, 2022.
- [5] R. Ogunsakin, N. Mehandjiev, and C. A. Marin, "Towards adaptive digital twins architecture," *Computers in Industry*, vol. 149, p. 103920, 2023.
- [6] E. Blasch, P. Schrader, G. Chen, S. Wei, Y. Chen, S. Khan, A. Aved, and A. Munir, "Dynamic digital twins for situation awareness," in *NAECON 2024-IEEE National Aerospace and Electronics Conference*. IEEE, 2024, pp. 433–440.
- [7] B. Wang, H. Zhou, X. Li, G. Yang, P. Zheng, C. Song, Y. Yuan, T. Wuest, H. Yang, and L. Wang, "Human digital twin in the context of industry 5.0," *Robotics and Computer-Integrated Manufacturing*, vol. 85, p. 102626, 2024.
- [8] J. Schulman, F. Wolski, P. Dhariwal, A. Radford, and O. Klimov, "Proximal policy optimization algorithms," *arXiv preprint arXiv:1707.06347*, 2017.
- [9] T. J. Ham, S. J. Jung, S. Kim, Y. H. Oh, Y. Park, Y. Song, J.-H. Park, S. Lee, K. Park, J. W. Lee *et al.*, "A³: Accelerating attention mechanisms in neural networks with approximation," in *2020 IEEE International Symposium on High Performance Computer Architecture (HPCA)*. IEEE, 2020, pp. 328–341.
- [10] E. E. Kosasih, E. Papadakis, G. Baryannis, and A. Brintrup, "A review of explainable artificial intelligence in supply chain management using neurosymbolic approaches," *International Journal of Production Research*, vol. 62, no. 4, pp. 1510–1540, 2024.
- [11] M. S. Munir, K. T. Kim, A. Adhikary, W. Saad, S. Shetty, S.-B. Park, and C. S. Hong, "Neuro-symbolic explainable artificial intelligence twin for zero-touch ioe in wireless network," *IEEE Internet of Things Journal*, 2023.
- [12] D. Ma, "Reinforcement learning and autonomous driving: Comparison between dqn and ppo," in *AIP Conference Proceedings*, vol. 3144, no. 1. AIP Publishing, 2024.
- [13] P. Aivaliotis, Z. Arkouli, K. Georgoulis, and S. Makris, "Methodology for enabling dynamic digital twins and virtual model evolution in industrial robotics—a predictive maintenance application," *International Journal of Computer Integrated Manufacturing*, vol. 36, no. 7, pp. 947–965, 2023.
- [14] T. G. Walmsley, P. Patros, W. Yu, B. R. Young, S. Burroughs, M. Apperley, J. K. Carson, I. A. Udugama, H. Aeowjaroenlap, M. J. Atkins *et al.*, "Adaptive digital twins for energy-intensive industries and their local communities," *Digital Chemical Engineering*, vol. 10, p. 100139, 2024.
- [15] W. J. Schmidt, D. Rincon-Yanez, E. Kharlamov, and A. Paschke, "Systematic literature review on neuro-symbolic ai in knowledge graph construction for manufacturing," *Semantic Web Journal TBD*, 2024.
- [16] B. Zhou, Z. Tan, Z. Zheng, D. Zhou, Y. He, Y. Zhu, M. Yahya, T.-K. Tran, D. Stepanova, M. H. Gad-Elrab *et al.*, "Neuro-symbolic ai at bosch: Data foundation, insights, and deployment," in *ISWC (Posters/Demos/Industry)*, 2022.
- [17] M. Jacob, L. Dierckx, and S. Nijssen, "Neurosymbolic ai: Combining deep learning and rule learning."
- [18] X. Ma, Q. Qi, J. Cheng, and F. Tao, "A consistency method for digital twin model of human-robot collaboration," *Journal of Manufacturing Systems*, vol. 65, pp. 550–563, 2022.
- [19] A. Ahmad, M. Kermanshah, K. Leahy, Z. Serlin, H. C. Siu, M. Mann, C.-I. Vasile, R. Tron, and C. Belta, "Accelerating proximal policy optimization learning using task prediction for solving games with delayed rewards," *arXiv preprint arXiv:2411.17861*, 2024.
- [20] T. Böttjer, D. Tola, F. Kakavandi, C. R. Wewer, D. Ramanujan, C. Gomes, P. G. Larsen, and A. Iosifidis, "A review of unit level digital twin applications in the manufacturing industry," *CIRP Journal of Manufacturing Science and Technology*, vol. 45, pp. 162–189, 2023.
- [21] J. Zhao, H. Feng, Q. Chen, and B. G. de Soto, "Developing a conceptual framework for the application of digital twin technologies to revamp building operation and maintenance processes," *Journal of Building Engineering*, vol. 49, p. 104028, 2022.
- [22] J. Renkhoff, K. Feng, M. Meier-Doernberg, A. Velasquez, and H. H. Song, "A survey on verification and validation, testing and evaluations of neurosymbolic artificial intelligence," *IEEE Transactions on Artificial Intelligence*, 2024.
- [23] Z. Wan, C.-K. Liu, H. Yang, R. Raj, C. Li, H. You, Y. Fu, C. Wan, S. Li, Y. Kim *et al.*, "Towards efficient neuro-symbolic ai: From workload characterization to hardware architecture," *IEEE Transactions on Circuits and Systems for Artificial Intelligence*, 2024.
- [24] Y. Chen, R. Cao, J. Chen, L. Liu, and B. Matsushita, "A practical approach to reconstruct high-quality landsat ndvi time-series data by gap filling and the savitzky-golay filter," *ISPRS Journal of Photogrammetry and Remote Sensing*, vol. 180, pp. 174–190, 2021.
- [25] S. Sharma, S. Tuli, and R. Paul, "Unsupervised learning of neuro-symbolic rules for generalizable context-aware planning in object arrangement tasks," in *2024 IEEE International Conference on Robotics and Automation (ICRA)*. IEEE, 2024, pp. 12 865–12 872.
- [26] M.-K. Leuven, "Problog 2: A probabilistic logic programming toolbox," 2023, available at <https://github.com/ML-KULeuven/problog>. [Online]. Available: <https://github.com/ML-KULeuven/problog>
- [27] S. Wang, J. Zhang, P. Wang, J. Law, R. Calinescu, and L. Mihaylova, "A deep learning-enhanced digital twin framework for improving safety and reliability in human-robot collaborative manufacturing," *Robotics and computer-integrated manufacturing*, vol. 85, p. 102608, 2024.
- [28] H. F. Coronel-Brizio, A. R. Hernández-Montoya, M. E. Rodríguez-Achach, H. Tapia-McClung, and J. E. Trinidad-Segovia, "Anderson-darling and watson tests for the geometric distribution with estimated probability of success," *PloS one*, vol. 19, no. 12, p. e0315855, 2024.
- [29] A. H. Victoria and G. Maragatham, "Automatic tuning of hyperparameters using bayesian optimization," *Evolving Systems*, vol. 12, no. 1, pp. 217–223, 2021.
- [30] T.-W. Weng, H. Zhang, P.-Y. Chen, J. Yi, D. Su, Y. Gao, C.-J. Hsieh, and L. Daniel, "Evaluating the robustness of neural networks: An extreme value theory approach," *arXiv preprint arXiv:1801.10578*, 2018.
- [31] X. Liu, H. Gan, Y. Luo, Y. Chen, and L. Gao, "Digital-twin-based real-time optimization for a fractional order controller for industrial robots," *Fractal and Fractional*, vol. 7, no. 2, p. 167, 2023.